



## Origin of the high variability of water mineral content in the bedrock aquifers of Southern Madagascar

V. Rabemanana<sup>a,b,\*</sup>, S. Violette<sup>a</sup>, G. de Marsily<sup>a</sup>, H. Robain<sup>b</sup>, B. Deffontaines<sup>c</sup>,  
P. Andrieux<sup>a</sup>, M. Bensimon<sup>d</sup>, A. Parriaux<sup>d</sup>

<sup>a</sup>UMR Sisyphe—Université Pierre et Marie Curie, case 123, 4 place Jussieu, 75252 Paris Cedex 05, France

<sup>b</sup>UR Géovast—Institut de Recherche pour le Développement, 32 avenue Henri Varagnat, 93143 Bondy, France

<sup>c</sup>Laboratoire de Géomorphologie et Environnement Littoral, EPHE 15 Boulevard de la mer, 35800 Dinard, France

<sup>d</sup>GEOLEP—Ecole Polytechnique Fédérale de Lausanne, 1015-Lausanne, Switzerland

Received 25 April 2003; revised 28 October 2004; accepted 12 November 2004

### Abstract

This study assesses the causes of the high spatial variability of the mineral content of groundwater in crystalline bedrock of Southern Madagascar. Although many kilometres from the coast and at a mean altitude of 400 m a.s.l., wells drilled in this area produce water with electrical conductivities in the range of 300–30,000  $\mu\text{S cm}^{-1}$  with a high spatial variability. Chemical and isotopic data are used to identify the processes involved in the groundwater mineralization. It is shown that the chemical composition of the groundwater in this region has its origin in (i) normal silicate and carbonate weathering reactions and (ii) input of marine salts, probably via rainfall recharge, modified by evapo-concentrative processes probably including precipitation and re-dissolution of secondary evaporites in the unsaturated zone. To obtain a better understanding of the spatial salinity distribution, well parameters such as yields, weathered zone thickness, weathered materials and morphological positions (upper slope, mid-slope, lower slope or valley bottom) are scrutinized.

A correlation was found between high salinity and low flow, shallow groundwater environments (flat hill tops, valley bottoms, weakly developed and clayey weathered zones) and between low salinity and high flow environments (granular, well-developed weathered zones and situation on valley slopes).

© 2005 Elsevier B.V. All rights reserved.

**Keywords:** Groundwater; Crystalline bedrock; Semi-arid climate; Hydrochemistry; Salinity; Water wells; Madagascar

### 1. Introduction

The southern part of Madagascar suffers from an acute lack of water. In 1990 and 1991, this region, especially the area around Androy, experienced a severe drought which decimated the population and the herds of zebus that constitute its wealth. To cope

\* Corresponding author. Present address: Centre d'Hydrogéologie—Université de Neuchâtel, Rue Emile Argand 11, CH-2007 Neuchâtel, Switzerland. Fax: +41 32 718 26 03.

E-mail address: [vero.rabemanana@unine.ch](mailto:vero.rabemanana@unine.ch) (V. Rabemanana).

with this dramatic situation, UNICEF financed a project which aimed at drilling and equipping with hand pumps around 150 wells for village water supplies. Twelve existing wells were repaired and re-used, thanks to this project. The BRGM (French geological survey) heading the program was faced with two difficulties: the low yields and the high mineral content in the water. Of the 217 new wells that were drilled (Fig. 1), 25% produce water too saline for drinking and agricultural use (i.e. electrical conductivities (EC) higher than  $3000 \mu\text{S cm}^{-1}$ , even reaching  $30,000 \mu\text{S cm}^{-1}$ ). These wells were plugged and abandoned. Overall, 64% of the 217 wells were equipped with hand pumps. The remaining 11% yielded less than  $0.5 \text{ m}^3 \text{ h}^{-1}$  (BRGM, 1995) and were not equipped.

Unfortunately, the hydrogeology and water chemistry in this region is poorly understood most studies are very limited and do not permit groundwater mineral concentrations to be examined (Aurouze, 1959;

Nicolini, 1983). Aurouze (1959) observed that in some of the bedrock-aquifer wells, the chloride content exceeded  $10 \text{ g L}^{-1}$ .

In previous studies, high mineral and chloride contents in the water of bedrock aquifers have been reported from Africa without any precise cause having been identified. Hypotheses have been formed concerning their origin: evaporation and dissolution (Savado, 1984; Travi and Mudry, 1997; Adams et al., 2001), contributions by rainwater and salt spray (Akiti, 1980), hydrothermal origin (Traoré, 1985), long residence time (Wright, 1992) and ultrafiltration in the clayey weathered layers (Kay, 1987).

The purpose of the present study is to identify the source(s) of the high distribution variability of groundwater mineral content in the bedrock aquifers in southern Madagascar. To this end, water chemistry characteristics and processes involved in groundwater mineralization are scrutinized. This study is the first of its kind dealing with the crystalline area of southern

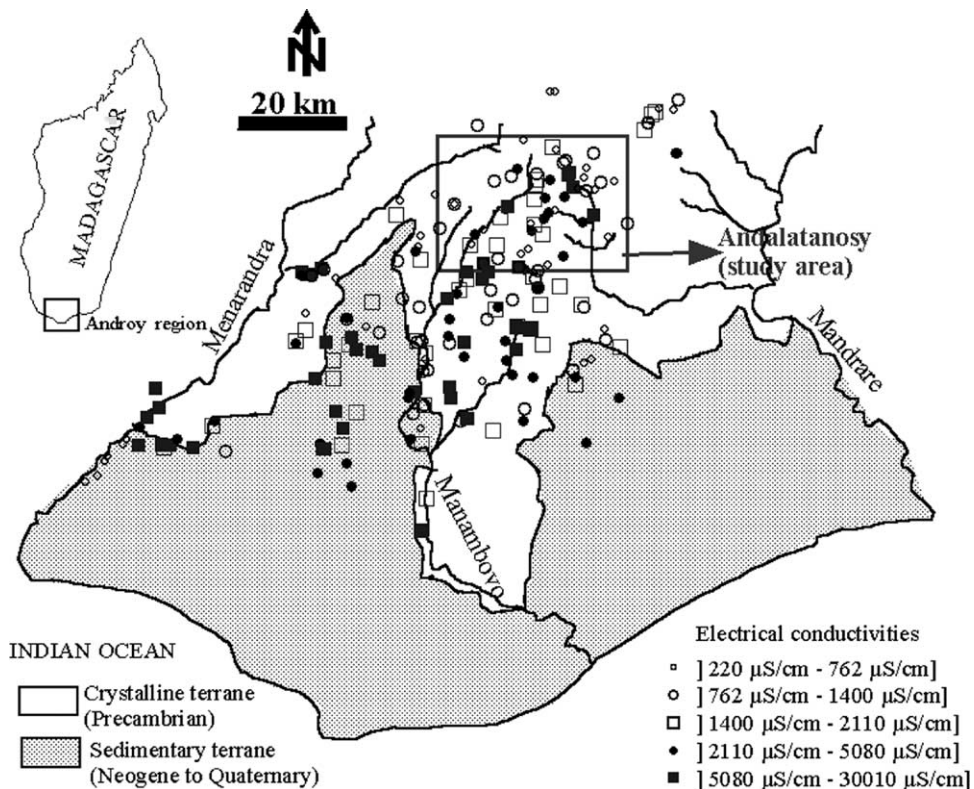


Fig. 1. Map of the southern Madagascar illustrating the distribution of electrical conductivities (EC) of the 217 wells and the location of the study area.

Madagascar. The results are expected to help solve the problem of the bedrock aquifers in this region and also to contribute to a better understanding of the bedrock hydrogeology in semi-arid and arid regions.

## 2. Geography and geology

The Androy area covers approximately 16,000 km<sup>2</sup> of southern Madagascar. Due to the shortcomings of the local infrastructures and to the difficulty of access in this area, our study is focused on a limited sector considered to be representative of the high spatial variability of the water mineral contents. The zone located upstream of the catchments of the rivers Menarandra, Manambovo and Mandrare, covering an area of 1200 km<sup>2</sup>, was selected (Fig. 1). Situated many kilometres from the coast, this area is a peneplain with an average altitude of 400 m a.s.l., within which erosion has left residual relief such as inselbergs. The mean annual rainfall is 600 mm, the potential evapotranspiration is about 1000 mm yr<sup>-1</sup> (Chaperon et al., 1993). The rivers, like most rivers in southern Madagascar, are ephemeral, with flow occurring but flow only in the rainy season between January and March. The vegetation is predominantly thorny bush typical of the Androy region and a few scattered mango and tamarind trees.

The study area consists of Precambrian metamorphic rocks which have been strongly deformed during the Pan-African events between 580 and 530 Ma (Andriamarohafatra et al., 1990; Paquette et al., 1994). According to some authors (Martelat et al., 1997; Windley and Bridgwater, 1971; Pili et al., 1997), the major strain trends associated with the high metamorphic grade are large shear zones with sub-vertical foliation oriented approximately N–S and complex elliptical and folded structures so-called ‘dome and basin’. The Precambrian rocks comprise various metamorphic lithologies: gneiss, leptynite, quartzite, schist and pyroxenite (Noizet, 1954; Lautel, 1958) and the shear zones may represent their lithological boundaries (Martelat et al., 1997; Ashwal et al., 1998). In addition to the classical constituent minerals of metamorphic rocks, there is an abundance of graphite associated with gneiss and schist, as well as phlogopite associated with pyroxenite (Lacroix, 1922; Lautel, 1958; Noizet, 1969).

## 3. Hydrogeology

The data set from 58 wells drilled in the study area reveals its hydrogeological conditions. The groundwater quality varies widely between the wells. No data are available on the variation of water salinity with depth. The aquifer system generally comprises a fractured, poorly weathered zone overlain by weathered regolith. The wells were often cased throughout the regolith, with open sections only in the bedrock. Regolith acts as a groundwater store which ultimately feeds the fracture systems tapped by the wells. The availability of groundwater depends on the presence and extent of the weathered zone cover and the presence of joints and fractures in the bedrock. The thickness of the weathered zone ranges from 2 to 45 m. Its lateral extent has been determined from geophysical investigations carried out in this study. Two geo-electrical images representative of results obtained from wells with high and low EC waters, respectively, are illustrated in Fig. 2. Generally, there is a good correlation between the water quality and the geometry of the aquifers. Wells with low EC were drilled in well-developed aquifers with large lateral extent and a thick weathered zone. However, a few wells that diverge from this coherence demonstrate that the aquifer geometry is not an exclusive discriminating factor in the spatial variability of the water salinity in the study area.

The water inflows occur mainly from fissures and fractures, typically at a depth of 10–20 m. Well yields range from 0.05 to 10.2 m<sup>3</sup> h<sup>-1</sup>. No significant correlation can be established between the bedrock lithology and the well yields. The median yield for the whole data set was 1.5 m<sup>3</sup> h<sup>-1</sup>. The highest yield was found in wells drilled in a valley bottom and the highest median yield occurred in wells situated at mid-slope.

Possible correlations have been examined between groundwater salinity and dominant fracture zone orientation, as determined from aerial and satellite images. No strong significant correlation was found, although there were weak indications that low yields and elevated groundwater mineralization were associated with the proximity to sub-meridional discontinuities, an observation which might warrant further, more rigorous studies.

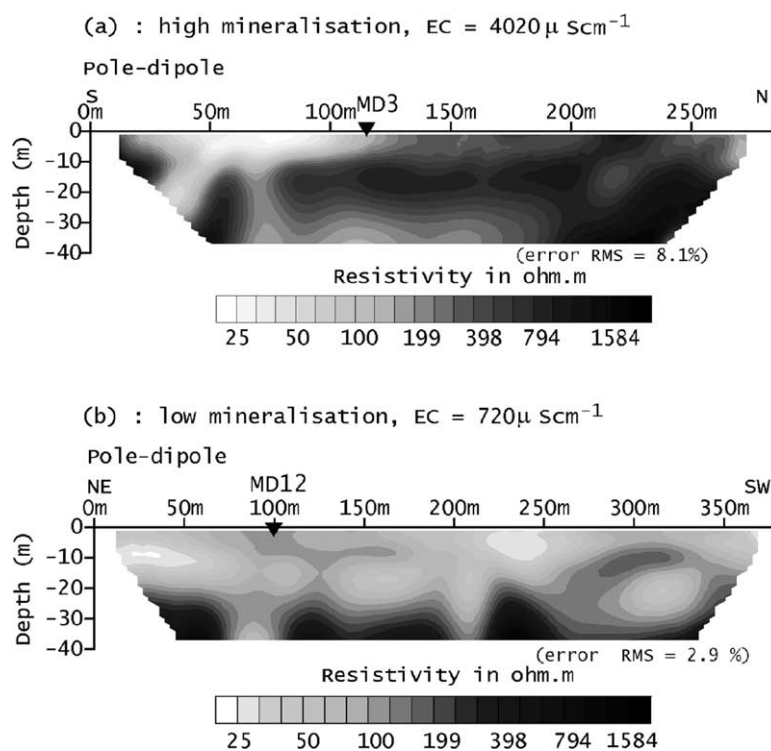


Fig. 2. Examples of geoelectrical images of the subsurface showing the geometry of the aquifers in the study area. Note the location of these two wells. The well MD12 which provides water with low electrical conductivity (EC) exploits well-developed aquifers formed by a thick weathered zone (thickness = 20 m,  $\rho < 80 \Omega\text{m}$ ) and a fractured zone corresponding to a large quasi-vertical conductive anomalies within a resistive bedrock ( $\rho > 400 \Omega\text{m}$ ).

Transmissivities vary between  $10^{-6}$  and  $10^{-3} \text{m}^2 \text{s}^{-1}$ . Among the 58 wells, 45 wells are equipped by hand pumps for the villagers' water supply.

#### 4. Hydrochemistry and isotopic characterisation

##### 4.1. Sampling and analysis

Twenty-four wells ranging in depth from 20 to 60 m were sampled in addition to seven other ones situated upstream and downstream from the studied area. These seven wells (MD200, MD201, MD202, MD300, MD400, MD401, MD500) make it possible to assess the representativeness of the selected area for the spatial heterogeneity distribution of the mineral contents in the water. Groundwater was collected after purging the wells for 15–20 min. Samples were filtered in the field with a 0.1  $\mu\text{m}$  membrane.

Unfiltered samples were collected for isotope analysis. In 10 wells, the activities of  $^{14}\text{C}$  and  $\delta^{13}\text{C}$  were measured.

The measurements of physical and chemical parameters (pH, T, EC) and that of alkalinity by titration with HCl 0.1 M were made in the field. The concentrations of  $\text{Ca}^{2+}$ ,  $\text{Mg}^{2+}$ ,  $\text{Na}^+$  and  $\text{K}^+$  were measured by flame absorption. The concentrations in  $\text{Cl}^-$ ,  $\text{SO}_4^{2-}$ ,  $\text{NO}_3^-$ ,  $\text{Br}^-$ ,  $\text{F}^-$  were measured by ionic chromatography and dissolved silica by colorimetry. The  $^{14}\text{C}$  activity was determined by a liquid scintillation technique. The results are reported as the percentage of the activity of modern carbon (pmc). Stable isotopic analyses ( $\delta^2\text{H}$ ,  $\delta^{18}\text{O}$  and  $\delta^{13}\text{C}$ ) were done using a mass spectrometer and the stable isotopic compositions are reported in  $\delta$  notation. The  $\delta^2\text{H}$  and  $\delta^{18}\text{O}$  values are given in per mil deviations from SMOW standard and  $\delta^{13}\text{C}$  from the Pee Dee Belemnite standard (PDB).

#### 4.2. Physical and analytical results

Analytical results are given in Table 1. They are related to samples collected in October 2000, at the end of the dry season when the water levels were at their lowest and the mineral contents in the water had reached their peak values. The temperature, EC and pH of the sampled water ranged between 25.3 and 28.5 °C, 437 and 5840  $\mu\text{S cm}^{-1}$ , and 7 and 8.28, respectively. The chemical and isotopic characteristics of the seven additional wells (MD200, MD201, MD202, MD300, MD400, MD401, MD500) are consistent with the other wells. The ion balance errors of the data set are acceptable within the 5% limit.

The major elements and EC distributions of the data set are in Fig. 3 illustrated with the cumulative frequency plots illustrated. A linearity of the frequency curve suggests a log-normality of the data distribution and the number of log-cycles on the x-axis is an indication of the variance of the data set (Banks et al., 1998).

The groundwater is characterized by high contents of  $\text{Na}^+$ ,  $\text{Cl}^-$  and alkalinity (Fig. 4). The concentrations of  $\text{Na}^+$  vary from 1.25  $\text{mmol L}^{-1}$  ( $\sim 29 \text{ mg L}^{-1}$ ) to 43.13  $\text{mmol L}^{-1}$  ( $\sim 992 \text{ mg L}^{-1}$ ) with a median of 8.52  $\text{mmol L}^{-1}$  ( $\sim 196 \text{ mg L}^{-1}$ ). The contents of  $\text{Cl}^-$  range from 0.75  $\text{mmol L}^{-1}$  ( $\sim 27 \text{ mg L}^{-1}$ ) to 41.94  $\text{mmol L}^{-1}$  ( $\sim 1489 \text{ mg L}^{-1}$ ) and the median concentration is 4.50  $\text{mmol L}^{-1}$  ( $\sim 160 \text{ mg L}^{-1}$ ). For the alkalinity, a variation of concentration from 2.74 to 12.58  $\text{meq L}^{-1}$  with a median of 6.55  $\text{meq L}^{-1}$  is observed. Almost all groundwaters have sodium as the dominant cation often followed by magnesium. The alkalinity (bicarbonate) is the dominant anion, but with increasing EC,  $\text{Cl}^-$  becomes more dominant with a relative abundance ( $> 60\%$  of the total anions) in the saline groundwaters ( $\text{EC} > 2500 \mu\text{S cm}^{-1}$ ).

#### 4.3. Water types and origin of dissolved ions

Based on the major ion contents, five dominant water types are identified and plotted in a Durov diagram (Fig. 5). They are:  $\text{Na-HCO}_3$ ,  $\text{Na-HCO}_3\text{-Cl}$ ,  $\text{Mg-HCO}_3$ ,  $\text{Na-Cl-HCO}_3$  and  $\text{Na-Cl}$ .

The dissolved ions in groundwater are mainly derived from three main processes:

- *Water rock interaction* (Freeze and Cherry, 1979; Hem, 1985). The most common water–rock interaction processes (weathering of silicates and carbonates) tend to release base cations (especially  $\text{Na}^+$  and  $\text{Ca}^{2+}$ ) and alkalinity ( $\text{HCO}_3^-$ ), whilst raising the pH. Subsequent ion exchange may modify the chemistry (especially the ratios of  $\text{Ca}^{2+}$  and  $\text{Na}^+$ ), while reactions such as oxidation of pyrite may prove to be a source of sulphate. The metamorphic nature of the bedrock of the study area precludes primary evaporite minerals such as gypsum or halite, which could be the sources of, e.g. chloride, sulphate or sodium.
- *The salt effect* essentially describes the evaporative concentration of solutes at the surface or in the shallow subsurface (Barica, 1972; Thomas et al., 1989; Nativ et al., 1997). This may include (i) evaporative concentration at the surface, (ii) concentration of solutes by evapotranspiration in the subsurface, (iii) precipitation and subsequent re-dissolution of secondary evaporite minerals in the unsaturated zone from evapo-concentrated waters. The solutes which are subject to this process may be derived from water–rock interaction (sodium, calcium, bicarbonate) or from external sources, such as marine salts (sodium, chloride, sulphate) arriving in the rainfall recharge. Inappropriate agricultural irrigation practices may significantly enhance the evapo-concentrative salt effect. Evapo-concentration will usually ultimately result in saturation with respect to mineral phases such as calcite: if the alkalinity exceeds calcium (as  $\text{meq L}^{-1}$ ), the calcium will be progressively removed from solution by further evapo-concentration, while the alkalinity will continue to increase.
- *Anthropogenic input*. Numerous studies (Girard and Hillarie-Marcelle, 1997; Travi and Mudry, 1997; Hudak, 1999; Jeong, 2001; Oren et al., 2004) have demonstrated that village waste tips, latrines, animal waste or manure/fertilisers can act as significant sources of e.g. nitrate, chloride, and potassium to groundwater. In semi-arid areas, the evapo-concentrative salt effect can increase the concentrations of these components to significant levels.

The plot of alkalinity vs [ $\text{Na}^+ + \text{K}^+ + \text{Ca}^{2+} + \text{Mg}^{2+}$ ] (Fig. 6) shows that almost all the waters fall below the equiline (1:1). This suggests another source

Table 1  
Chemical composition (in mmol L<sup>-1</sup>) and isotopic contents of the groundwater

Well	EC ( $\mu\text{S cm}^{-1}$ )	pH	Ca <sup>2+</sup>	Mg <sup>2+</sup>	Na <sup>+</sup>	K <sup>+</sup>	Alk (meq L <sup>-1</sup> )	NO <sub>3</sub> <sup>-</sup>	SO <sub>4</sub> <sup>2-</sup>	Cl <sup>-</sup>	Br <sup>-</sup>	F <sup>-</sup>	SiO <sub>2</sub>	B.I. (%)	Br/Cl	$\delta^{18}\text{O}$ (‰)	$\delta^2\text{H}$ (‰)	<sup>14</sup> C (% pcm)	$\delta^{13}\text{C}$ (‰)
MD2	437	7.00	0.22	0.36	3.24	0.07	2.74	0.08	0.30	0.85	0.002	0.025	1.16	2.29	$2.35 \times 10^{-3}$	-5.51	-36.1		
MD3	4020	7.33	2.98	6.77	21.39	0.24	7.31	8.35	2.70	20.76	0.030	0.023	0.80	-0.83	$1.45 \times 10^{-3}$	-4.97	-35.1	88.7	-13.47
MD4	1980	7.28	2.68	6.32	2.45	0.11	5.91	6.54	1.29	5.45	*	0.030	1.78	0.19		-5.07	-35.7		
MD5	1494	7.64	0.68	1.22	12.88	0.08	8.88	0.05	0.87	6.33	0.012	0.119	1.37	-0.71	$1.90 \times 10^{-3}$	-4.75	-34.3		
MD6	1132	7.04	0.55	1.33	8.52	0.08	6.28	0.60	0.66	4.08	0.005	0.034	1.31	0.32	$1.23 \times 10^{-3}$	-4.45	-31.8		
MD7	2180	7.15	1.71	3.20	13.09	0.07	8.31	1.33	1.38	10.92	0.017	0.051	1.18	-0.73	$1.56 \times 10^{-3}$	-4.96	-35.4	103.7	-13.00
MD8	1490	7.19	0.94	1.80	9.37	0.14	6.55	1.18	0.99	5.40	0.007	0.074	1.32	-0.40	$1.30 \times 10^{-3}$	-5.10	-35.8		
MD9	2240	7.59	0.44	1.23	15.44	0.03	9.32	0.15	1.04	7.55	0.003	0.113	1.20	-0.76	$3.97 \times 10^{-4}$	-4.87	-34.0		
MD10	757	7.91	0.08	0.16	7.54	0.02	5.93	0.34	0.16	1.34	0.012	0.150	1.26	0.69	$8.96 \times 10^{-3}$	-4.57	-34.1	104.7	-12.73
MD11	2040	7.65	0.96	2.17	15.14	0.05	10.81	0.47	1.58	7.25	0.007	0.126	1.63	-0.56	$9.66 \times 10^{-3}$	-4.10	-31.9	104.2	-10.90
MD12	720	7.90	0.79	1.16	7.65	0.14	5.81	0.37	0.55	4.27	0.003	0.026	1.50	0.60	$7.03 \times 10^{-3}$	-4.84	-34.0	103.6	-11.28
MD14	686	7.47	0.92	0.76	5.24	0.02	4.99	0.25	1.13	0.90	0.010	0.078	1.47	1.29	$1.11 \times 10^{-2}$	-5.18	-36.1		
MD15	1632	7.58	0.65	1.44	12.58	0.12	7.75	1.74	0.65	6.46	0.005	0.111	1.30	-1.08	$7.74 \times 10^{-3}$	-4.51	-32.8		
MD16	700	7.36	0.46	0.92	8.48	0.08	5.73	*	0.73	3.88	0.002	0.055	1.35	1.12	$5.15 \times 10^{-3}$	-5.41	-39.2		
MD17	555	7.33	0.83	0.77	2.77	0.04	4.87	0.02	0.15	0.75	0.003	0.035	1.35	0.59	$4.00 \times 10^{-3}$	-5.50	-37.3		
MD18	663	7.14	0.85	1.90	1.25	0.04	4.19	0.92	0.41	1.01	0.046	0.027	1.80	-1.09	$4.55 \times 10^{-3}$	-5.30	-37.4		
MD19	5300	7.42	1.88	4.10	43.13	0.12	10.36	0.02	4.44	35.59	0.002	0.131	1.19	0.33	$5.62 \times 10^{-5}$	-4.90	-34.1	69.1	-11.92
MD20	629	7.36	0.45	0.54	4.80	0.02	5.47	0.10	0.17	0.77	0.003	0.074	1.44	0.89	$3.90 \times 10^{-3}$	-5.09	-36.1		
MD21	790	7.48	0.58	1.13	5.07	0.01	6.27	0.27	0.18	1.36	0.058	0.063	1.51	1.43	$4.26 \times 10^{-2}$	-5.05	-34.7	112.6	-12.68
MD22	5840	7.22	6.43	8.85	33.25	0.24	6.73	*	7.10	41.94	0.004	0.040	1.00	0.93	$9.54 \times 10^{-5}$	-4.65	-33.6		
MD23	1272	8.28	0.11	0.18	13.61	0.04	11.02	0.05	0.36	1.97	*	0.132	1.72	1.68		-4.91	-35.8	94.9	-9.93
MD24	960	7.17	0.46	1.15	5.50	0.03	4.62	1.38	0.37	1.83	0.004	0.068	1.63	1.04	$2.19 \times 10^{-3}$	-4.88	-34.4		
MD50	1178	7.58	1.05	1.06	7.33	0.06	5.77	2.11	0.34	2.84	0.011	0.088	1.41	0.91	$3.87 \times 10^{-3}$	-4.70	-32.4		
MD100	2750	7.57	1.07	2.69	5.97	0.26	4.45	0.85	0.46	7.55	0.011	0.014	1.41	-0.07	$1.46 \times 10^{-3}$	-5.40	-36.8		
MD200	2340	7.70	0.83	1.29	20.30	0.06	12.58	0.31	1.76	8.03	0.003	0.206	1.62	0.33	$3.74 \times 10^{-4}$	-5.00	-35.4	102.6	-10.89
MD201	836	7.64	0.55	0.50	6.81	0.09	6.80	0.09	0.52	1.06	0.003	0.060	1.07	0.06	$2.83 \times 10^{-3}$	-5.60	-38.9		
MD202	2190	7.75	0.45	1.63	18.62	0.06	9.57	0.96	0.94	9.67	0.014	0.118	1.35	1.69	$1.45 \times 10^{-3}$	-4.50	-32.9	93.7	-11.50
MD300	915	7.52	1.62	1.17	3.25	0.06	3.92	0.06	0.74	3.27	0.014	0.028	1.52	0.91	$4.28 \times 10^{-3}$	-4.90	-37.1		
MD400	2350	7.47	1.45	2.88	16.35	0.19	9.04	4.96	1.76	7.41	0.006	0.110	1.35	0.54	$8.10 \times 10^{-4}$	-4.30	-30.4		
MD401	2870	7.45	1.53	2.51	21.80	0.18	11.03	0.43	2.42	13.52	0.022	0.086	1.51	0.40	$1.63 \times 10^{-3}$	-4.60	-31.5		
MD500	1330	7.06	1.65	2.06	6.29	0.14	7.06	0.10	1.20	4.50	0.005	0.027	1.39	-0.75	$1.11 \times 10^{-3}$	-5.40	-36.1		

\* , Below detection limit; BI, ionic balance error (%); Br/Cl, molar ratio;  $\delta^{18}\text{O}$ ,  $\delta^2\text{H}$ , in ‰ vs SMOW; <sup>14</sup>C, in % pcm;  $\delta^{13}\text{C}$ , in ‰ vs PDB.

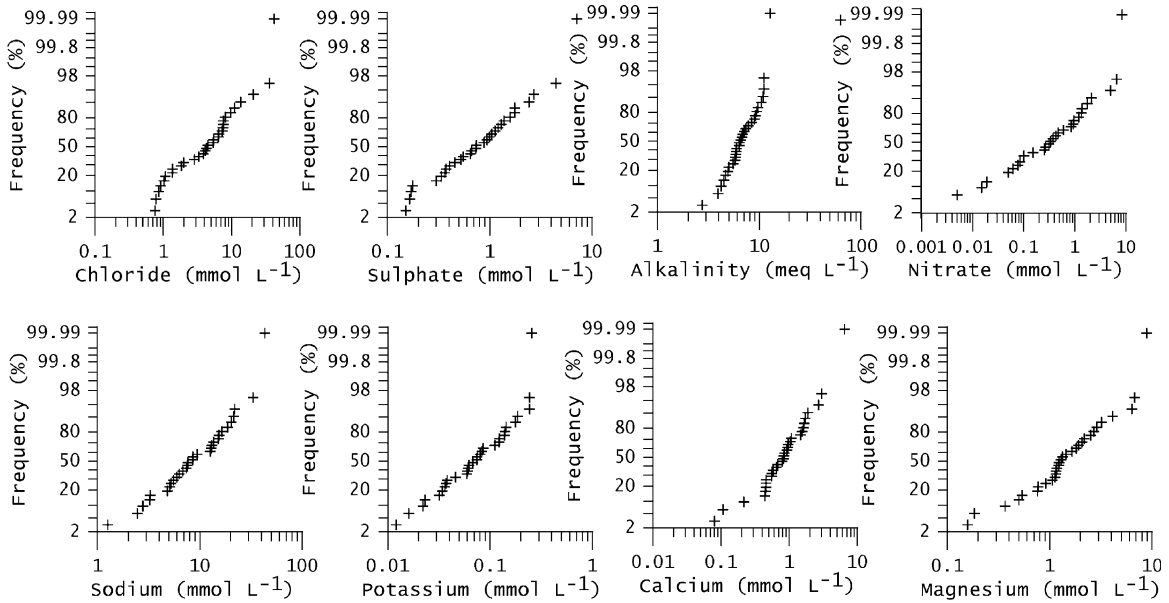


Fig. 3. Cumulative frequency diagrams for major ions ( $N=31$ ). Note logarithmic  $x$ -axis and probability scale on  $y$ -axis. A linearity of these curves indicates a log-normality of the data distribution.

of cations in addition to water–rock interaction processes.

Fig. 7 illustrates the significant correlation between the  $\text{Na}^+$  and  $\text{Cl}^-$  ions, which indicates that the major part of the salinity in the groundwater is due to salt. This reflects the salt effect as a partial source of  $\text{Na}^+$  ions in addition to silicate weathering and ion exchanges. The observed excess of  $\text{Na}^+$  over  $\text{K}^+$

for our data set is due to the greater resistance of  $\text{K}^+$  to weathering and its fixation in neo-formation minerals. Calcium and magnesium concentrations show a significant correlation due largely to silicate

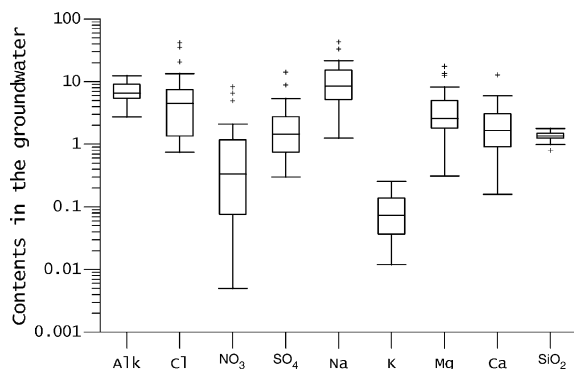


Fig. 4. Boxplot illustrating the distribution of selected parameter concentrations in the groundwater. All contents are given in  $\text{meq L}^{-1}$  except that of  $\text{SiO}_2$  in  $\text{mmol L}^{-1}$ . The box represents the interquartile of the data set with a horizontal line at the median. Outlying data points are represented by crosses,  $N$  (number of analyses) = 31 for each boxplot.

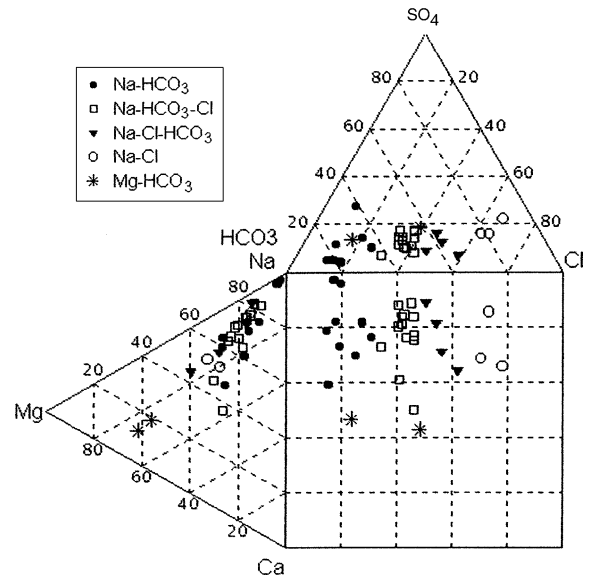


Fig. 5. Durov diagram showing the main water types in the study area according to their  $\text{meq L}^{-1}$  ionic proportions, nitrate and potassium are omitted from the presentation.

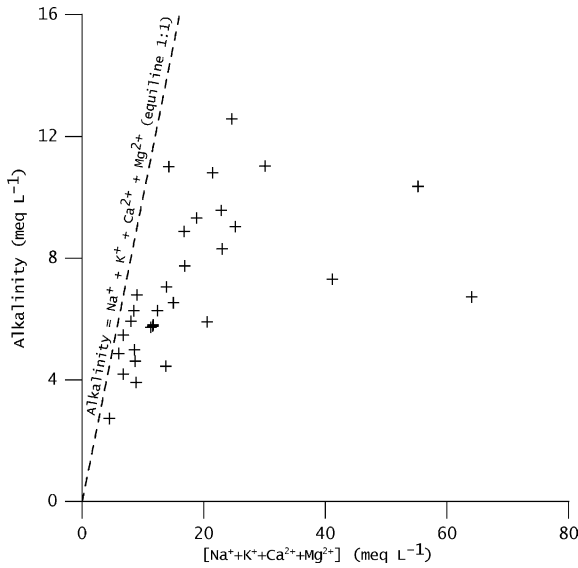


Fig. 6. x-y plot of alkalinity vs  $[Na^+ + K^+ + Ca^{2+} + Mg^{2+}]$ . All data set are below the equiline (1:1).

and carbonate weathering. Most groundwater samples have a concentration of  $Mg^{2+}$  much higher than that of  $Ca^{2+}$ . This may be explained by the abundance of ferromagnesian minerals present within the rocks of the area, by ion exchange processes and by the precipitation of calcite.

The plot of  $SO_4^{2-}$  vs  $Cl^-$  illustrates the strong correlation between these ions suggesting that their accumulation in the groundwater is a result of a common process (evapo-concentration or dissolution of secondary evaporite minerals). Other source of  $SO_4^{2-}$  ions may also be the oxidative weathering of

pyrite which are associated with pyroxenic facies and/or the dissolution of anhydrite.

### 5. Origin of the salinity

The climate, the geological setting and the significant correlations between various major elements and the EC (Fig. 8) leads to several possible sources of salinity in the study area.

#### 5.1. Water-rock interaction

Two processes can be proposed as probable sources of salinity from water-rock interactions, namely leaching of fluid inclusions and mineral weathering. According to Nordstrom and Olsson (1987), salinization from fluid inclusion leakage requires minimum porosities and static groundwater conditions. Due to the use of the wells as water supply and the transmissivity values of some of them (about  $10^{-4} m^{-2} s^{-1}$ ), the hydraulic conditions of the groundwater in this area are not static. Among the rocks present in the region, pyroxenite contains minerals that may be a source of  $Cl^-$ . Its mineralization is characterized by the association of minerals such as: phlogopite, pyroxene, pyrite, azurite, calcite, apatite, sphene, anhydrite, fluorite, spinel, actinolite, pyrrhotite, thorianite, zircon, anorthite and scapolite (Lacroix, 1922; Lautel, 1958).

Weathering of phlogopite and scapolite is probably a partial source of groundwater salinity from water-rock interaction. These minerals are abundant in the region. High EC values of 17,000, 6000 and

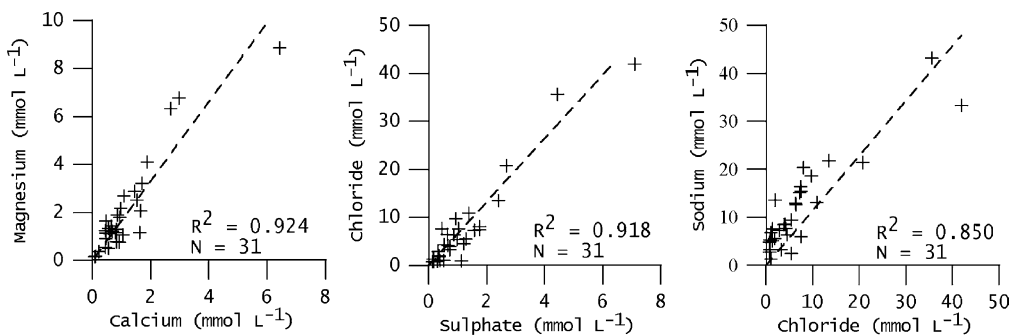


Fig. 7. x-y plot illustrating the correlation between major ions (magnesium vs calcium, chloride vs sulphate, sodium vs chloride).



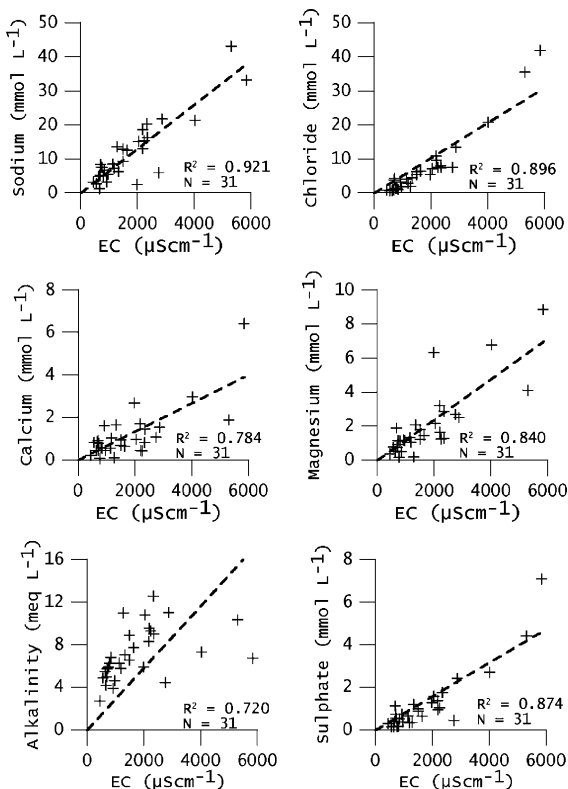


Fig. 8.  $x$ - $y$  plot illustrating the correlation between electrical conductivities (EC) and major ions.

$5500 \mu\text{S cm}^{-1}$  were observed in the wells situated close to the phlogopite quarries and chloride concentrations as high as  $17 \text{ g L}^{-1}$  reported by Aurouze (1959) from water drawn from other mica mines in southern Madagascar bear out this assumption.

## 5.2. Evaporation and salt dissolution

Table 1 shows that  $\delta^{18}\text{O}$  values range from  $-5.6$  to  $-4.1\text{‰}$  and that  $\delta^2\text{H}$  values vary between  $-39.2$  and  $-30.4\text{‰}$ . No significant difference was observed between samples with low and high salinity. Fig. 9 plots the stable isotopic compositions ( $\delta^2\text{H}$ ,  $\delta^{18}\text{O}$ ) together with the global meteoric water line (GMWL) (Craig, 1961). Compared to the GMWL, all samples are depleted in deuterium and lie on a regression line with a slope of 5.05. This depletion indicates that the groundwater has been subjected to evaporation before or during infiltration. The plot of alkalinity vs

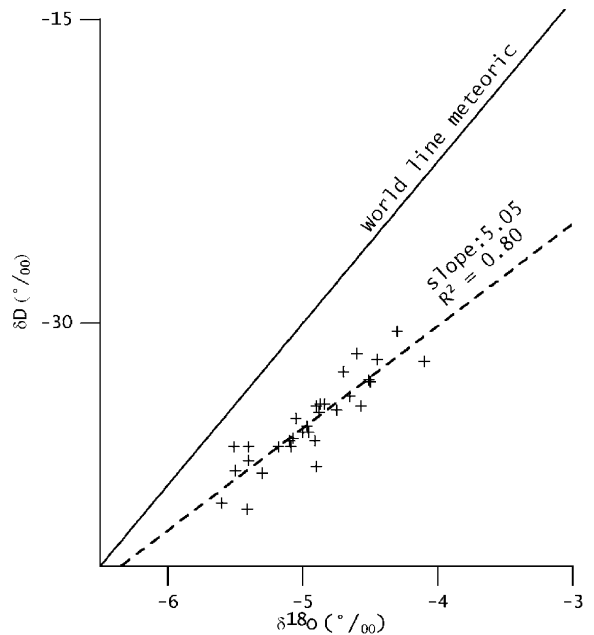


Fig. 9.  $x$ - $y$  plot of stable isotopic composition together with GMWL. All water samples are depleted in deuterium.

$[\text{Cl}^- + \text{SO}_4^{2-}]$  (Fig. 10) shows that some points are close to or on the line 1:1. This demonstrates an accumulation of alkalinity, chloride and sulphate as a result of common processes such as evapo-concentration or dissolution of salt. The fact that most saline samples fall below the equiline may indicate some limit on the accumulation of alkalinity (e.g. calcite precipitation).

## 5.3. Marine contribution

The existence of a marine Br/Cl ratio in many samples (MD3, MD5, MD8, MD100, MD202, MD401) indicates a marine origin for both these anions. The recent age of the waters (as evidenced by relatively high  $^{14}\text{C}$  activities), the lack of any plausible tectonic or geomorphological evidence for recent seawater intrusion at the current altitude (400 m a.s.l.) and the apparent stability of the present altitude (Battistini, 1970), all argue against direct seawater intrusion and for marine salt incorporation into rainfall recharge, as the source of these marine ions. Br/Cl ratios which are lower than the marine ratio in some wells may reflect subsurface

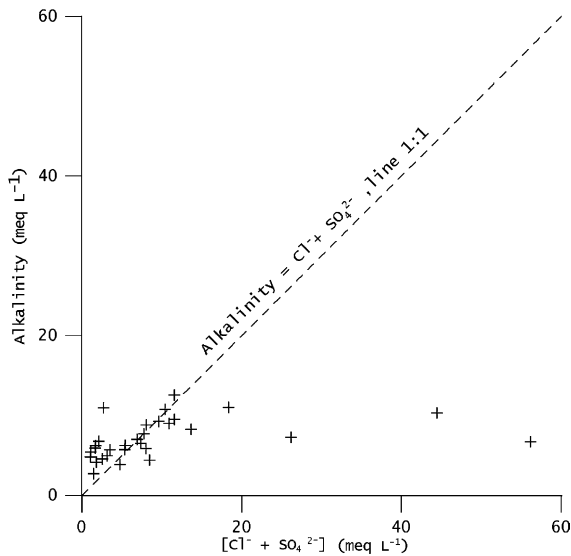


Fig. 10.  $x$ - $y$  plot of alkalinity vs  $[\text{Cl}^- + \text{SO}_4^{2-}]$ . This curve could demonstrate mutual accumulation of alkalinity, chloride and sulphate by a common process (evapo-concentration or dissolution of secondary evaporite minerals).

fractionation due to possible precipitation and re-dissolution of secondary evaporites in the unsaturated zone.

#### 5.4. Human activities

High nitrate contents exceeding World Health Organization (WHO) drinking water guidelines limited to  $0.72 (\text{NO}_3^-) \text{ meq L}^{-1}$  ( $\sim 45 \text{ mg L}^{-1}$ ) were detected in some water samples. In a previous study, De Robillard (1949) already observed high nitrate concentrations in the groundwater of southern Madagascar. When examining the data collected in the present study, one finds no significant correlation between  $\text{Cl}^-$  and  $\text{NO}_3^-$  ions (Fig. 11). However, it was observed that irrigated agriculture (mainly vegetables) is located in the vicinity of wells and that the high  $\text{NO}_3^-$  concentrations are found in wells drilled downstream of the villages and/or the latrine zones. Groundwater provides the water needed for the production of vegetables in the region. The occurrence of high nitrate contents in the groundwater may be attributed to domestic wastewater and/or recycling of salts from irrigation.

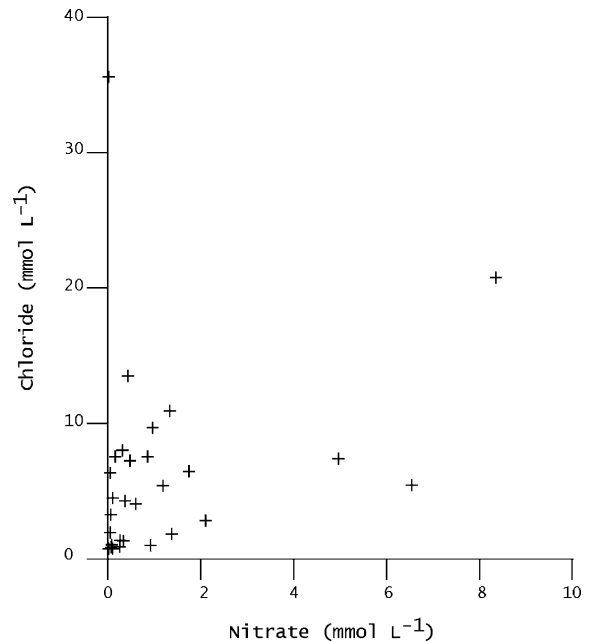


Fig. 11.  $x$ - $y$  plot of  $\text{Cl}^-$  vs  $\text{NO}_3^-$ . No clear correlation is observed between these ions.

### 6. Co-variation of salinity with other parameters

In order to better understand the spatial distribution of the groundwater salinity in the study area, a multivariate statistical analysis was performed with well parameters, i.e. geomorphological positions, well yields ( $Q$ ), weathered zone thickness ( $E$ ), elevation (Alt) and weathered materials. Here the multivariate analysis was carried out by combining multiple-correspondence analysis and cluster analysis for 58 wells in the study area. The wells were distributed with respect to their morphological settings: top of the hill (TH), upper part of the hill slope (UH), middle of the hill slope (MH), foot of the hill slope (FH) and valley bottom (VB). Quantitative variables ( $EC$ ,  $E$ , Alt,  $Q$ ) were split into intervals containing the same number of data. This avoids distortion of data without deforming the information stored in the original data set (Escofier and Pagès, 1998). The limits of each interval are given in Table 2. Qualitative parameters of wells (weathered materials) considered as supplementary variables are not taken into account in the calculation of the factorial axis. They are projected on the factorial plane in order to determine if a general

Table 2  
Limits defining the intervals of the quantitative variable of the wells

Variable	Class	Range
Electrical conductivity EC ( $\mu\text{S cm}^{-1}$ )	1	270–1000
	2	1000–2000
	3	2000–17000
Well yield ( $\text{m}^3 \text{h}^{-1}$ )	1	0.05–1
	2	1–2
	3	2–4
	4	4–10
Thickness of weathered zones (m)	1	2.6–10
	2	10–13.5
	3	13.5–28.6
Elevation (m)	1	310–350
	2	310–390
	3	390–400
	4	400–450

trend exists. Then, the cluster analysis is applied to factors. This approach permits us to reduce a classification error due to the multicollinearity of the data (Suk and Lee, 1999).

The results of this statistical analysis are shown on a dendrogram (Fig. 12). It was noted that local factors in the surrounding of wells influence the groundwater salinity and its spatial distribution. Wells producing saline water are associated with low yields and installed in areas with a thin weathered layer. The weathered materials are of a clay type. These wells are situated at the top of the thalwegs (plateaus) or on the valley bottom. Fresh water is produced by wells installed in the upper part of the hill slope or at mid-slope of a thalweg. The yields are high. The weathered

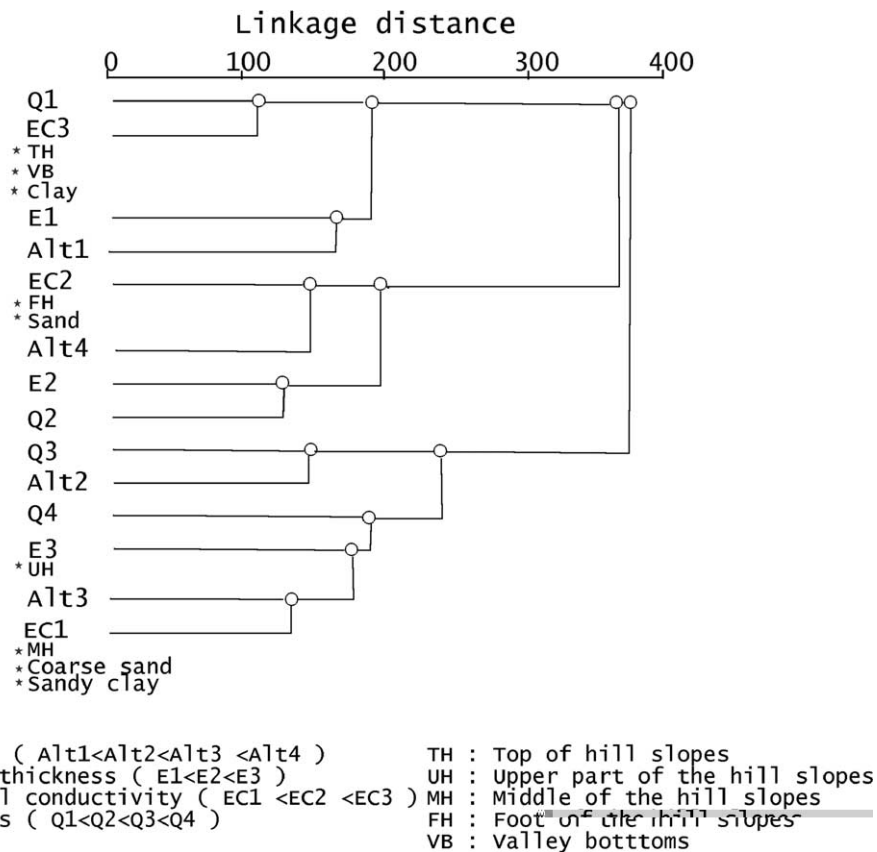


Fig. 12. Dendrogram of cluster analysis illustrating the links between the groundwater salinity and the well parameters. Saline waters (EC 3) are associated with well parameters such as: low yields (Q1), situation at the top of hill slope (TH) or on a valley bottom (VB), thin weathered layer (E1). Fresh waters (EC1) are extracted from wells associated with high yields (Q3, Q4), an installation in the upper slope (UH) or at mid-slope (MH) and thick weathered zones (E3).

zones are thick and formed by sandy clay or coarse sand.

### 7. General discussion

In the bedrock aquifers of southern Madagascar, the accumulation of groundwater salinity is multiple. Its highly variable distribution may be related to various factors: geometry of the aquifer, fracture apertures, morphological setting of the wells, weathering products, chemical features of the water. Taking into account these factors, a conceptual aquifer model explaining the processes involved in mineralizing the water in the study area is proposed (Fig. 13).

#### 7.1. On the flat hill

Due to the clayey nature of the weathered zones, infiltration is difficult. The shallow depth of the water level and the low velocity of the circulating water favour groundwater loss by evaporation and salt accumulation in the unsaturated zone. In parallel, as velocities are small and the water transit time long, water–rock contact is probably increased leading to dissolution and reactions with the aquifer matrix. Wells installed on the plateaus tend to produce very mineralized water.

#### 7.2. On the hill slopes

The coarse and sandy clay of the weathered zone in conjunction with the topographical slope allow percolation and lateral flow. A hydraulic connection may exist between the shallow and deep aquifers. Loss by evaporation and leaching of salts is relatively small. Generally, the water withdrawn from wells situated in the upper parts of the slopes and at mid-slope have low mineral contents, especially in fracture zones.

#### 7.3. On the valley bottom

Here, the thickening of the weathered zones and the greater degree of fissuring and fracturing combine to increase aquifer reservoirs. Infiltration depends on the amount of clay contained in the weathered zone. In this morphological unit, losses by evaporation and salt deposits increase. The majority of wells drilled in the valley bottoms and depressions produce saline water which is attributed to dissolution of salts accumulated at the subsurface by evaporation.

The effects of human activities as well as those resulting from alteration of phlogopite and scapolite minerals (in the vicinity of the occurrence of such minerals, e.g. near mica quarries) are superimposed on this functioning pattern.

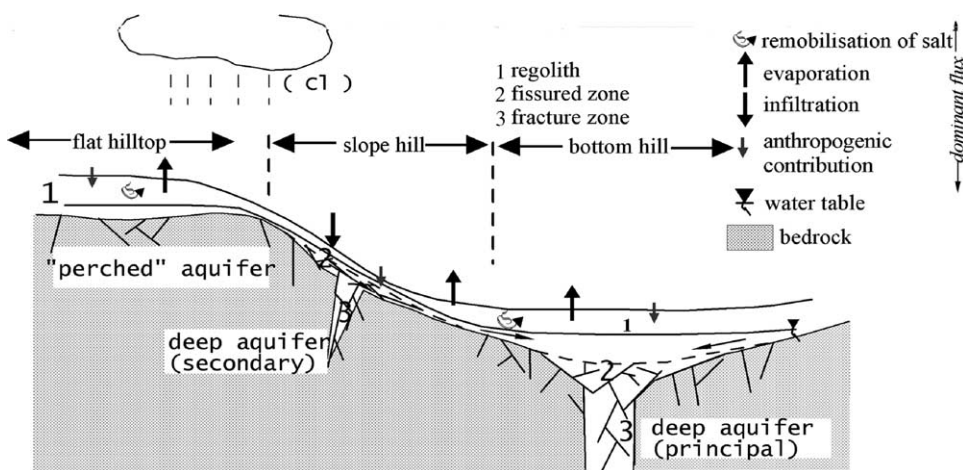


Fig. 13. Conceptual aquifer model explaining the processes involved in mineralizing the water. The main sources of salinity are reported taking into account the topographical units and the type of aquifer.

## 8. Conclusions

The groundwater quality in the bedrock aquifer of southern Madagascar has a large spatial variability. This may reflect on the one hand the interplay of various processes involving groundwater mineralization and on the other the regionally weak hydraulic connectivity between aquifer systems. In this study, samples of the rainfall are not available and its dissolved ion contents are not determined. In any case, the salt input from the rainfall alone cannot explain the total and the highly variable distribution of groundwater salinity. The main processes governing the groundwater chemistry in this region are: (i) normal silicate and carbonate weathering reactions and (ii) input of marine salts, probably via rainfall recharge, modified by evapo-concentrative processes including probably precipitation and re-dissolution of secondary evaporites in the unsaturated zone. The occurrence of high nitrate concentrations in wells vulnerable to human activities was observed. The impact of these processes is modified by local topographic and hydrogeological conditions. Accumulation of salts by evaporation occurs mainly in topographically lower or flatter areas. Whenever the recharge takes place, it leaches soluble salts in the unsaturated zone. The multivariate analysis performed with well parameters allows to a better understanding of the spatial distribution of the salinity in this region. It was found that high salinity is associated with low flow and shallow groundwater environments (flat hill tops, valley bottoms, weakly developed and clayey weathered zones) and low salinity is related to high flow environments (granular, well-developed weathered zones, situated on valley slopes).

This study was carried out thanks to the collaboration between the Institut de Recherche pour le Développement (IRD) and the Institut et Observatoire Géophysique d'Antananarivo (IOGA) within the CAMPUS program financed by the French Ministry for Foreign Affairs (MAE) and with the assistance of the CNRS-INSU (National Institute for Sciences of the Universe, project PNRH-99).

The authors are grateful to Alexei Bobachev, Jacques Boulègue, Jean-Paul Deroin, Eddy Rasolomanana for their contributions during fieldwork. Thanks to Yves Albouy, Laurent Dewindt, Jean-Claude Macquar, Jean-Luc Michelot, Bernard Moine,

Jean Bruno Ratsimbazafy, Jean-Paul Sagon for their fruitful discussion.

All laboratory staff who contributed to the chemical and stable isotope analyses is warmly thanked.

Thanks to David Banks and an anonymous reviewer for their helpful comments on an earlier draft of our manuscript.

## References

- Adams, S., Titus, R., Pietersen, K., Tredoux, G., Harris, C., 2001. Hydrochemical characteristic of aquifers near Sutherland in the Western Karoo, South Africa. *J. Hydrol.* 241, 91–103.
- Akiti, T.T., 1980. Etude géochimique et isotopique de quelques aquifères du Ghana: gneiss de la plaine d'Accra, calcaires de la plaine au Sude Est de la Volta, granites de la Hautes région. Doctoral Thesis. University of Paris Sud Orsay, p. 232.
- Andriamarohafatra, J., de La Boisse, H., Nicollet, C., 1990. Datation U–Pb sur les monazites et zircons du dernier épisode tectono-métamorphique granulitique majeur dans le Sud Est de Madagascar. *C. R. Acad. Sci. (Paris)* 310, 1643–1648.
- Ashwal, L.D., Hamilton, M.A., Morel, V.P.I., Rambelison, R.A., 1998. Geology, petrology and isotope geochemistry of massif-type anorthosite from southwestern Madagascar. *Contrib. Miner. Petrol.* 133, 389–401.
- Aurouze, J., 1959. Hydrogéologie du Sud de Madagascar. Doctoral Thesis. University of Paris, p. 191.
- Banks, D., Frengstad, B., Midtgard, A.K., Krog, J.R., Strand, T., 1998. The chemistry of Norwegian groundwaters: I. The distribution of radon, major and minor elements in 1604 crystalline bedrock groundwaters. *Sci. Total Environ.* 222, 71–91.
- Barica, J., 1972. Salinization of groundwater in arid zones. *Water Res.* 6, 925–933.
- Battistini, R., 1970. Etat des connaissances sur les variations du niveau marin à Madagascar depuis 10 000 ans. *C. R. Sem. Géol. Mad.* 1970, 13–15.
- BRGM, 1995. Programme d'hydraulique villageoise: 150 points d'eau dans le Sud de Madagascar. Rapport de fin de travaux no. 1976 MDB/SGN/95, p. 40.
- Chaperon, P., Danloux, J., Ferry, L., 1993. Fleuves et Rivières de Madagascar, Editions Orstom 1993, p. 897.
- Craig, H., 1961. Isotopic variation in meteoric waters. *Science* 133, 1702–1703.
- De Robillard, R., 1949. La présence de nitrates dans les eaux de puits du Sud-Ouest et du Sud de Madagascar. *Bull. Géol. Mad.* 1949, 88–90.
- Escofier, B., Pagès, J., 1998. Analyses Factorielles Simples et Multiples: Objectifs, Méthodes et Interprétation, 3ème Edition, Dunod Paris 1998 p. 284.
- Freeze, R.A., Cherry, J.A., 1979. *Groundwater*. Prentice-Hall, Englewoods Cliff, NJ p. 604.

- Girard, P., Hillarie-Marcelle, C., 1997. Determining the source of nitrate pollution in the Niger discontinuous aquifers using the natural  $^{15}\text{N}/^{14}\text{N}$  ratios. *J. Hydrol.* 199, 239–251.
- Hem, J.D., 1985. Study and interpretation of the chemical characteristics of natural water. USGS Water Supply Paper 2254, p. 253.
- Hudak, P.F., 1999. Chloride and nitrate distributions in the Hickory aquifer, central Texas, USA. *Environ. Int.* 25, 393–401.
- Jeong, C.H., 2001. Effect of land use and urbanization on hydrochemistry and contamination of groundwater from Taejon. *Korean J. Hydrol.* 253, 194–210.
- Kay, R.L.F., 1987. Hydrochemistry applied to development of crystalline bedrock aquifers. *Groundwater Exploration and Development in Crystalline Basement Aquifers, Proceedings, Zimbabwe, June 1987, II-7*, pp. 71–89.
- Lacroix, A., 1922. *Minéralogie de Madagascar, Tome 1*, Challamal eds. Paris 1922, p. 603.
- Lautel, R., 1958. Etude géologique de la feuille de bekistro. *Trav. Bur. Géol.* 4, 33 (Service Géologique Tananarive).
- Martelat, J.E., Nicolle, C., Lardeaux, J.M., Vidal, G., Rakotondrazafy, R., 1997. Lithospheric tectonic structures developed under high-grade metamorphism in southern part of Madagascar. *Geodin. Acta* 10, 94–114.
- Nativ, R., Adar, E., Dahan, E., Nissim, I., 1997. Water salinization on arid regions—observations from the Negev desert. *Isr. J. Hydrol.* 196, 271–296.
- Nicolini, E., 1983. Bilan des résultats géochimiques tirés de l'études des nappes de l'extrême sud de Madagascar. *Mad. Rev. Géol.* 42, 41–57.
- Noizet, G., 1954. Etude géologique des schistes cristallins des feuilles Imanombo—Ranomainty—Tranomaro—Marohotro. *Trav. Bur. Géol.* 57, 90 (Service Géologique Tananarive).
- Noizet, G., 1969. Sur l'origine et la classification des pyroxénites Androyennes du Sud de Madagascar. *C. R. Sem. Géol. Mad.* 1969, 155–159.
- Nordstrom, D.K., Olsson, T., 1987. Fluid inclusions as a source of dissolved salts in deep granitic groundwaters. In: *Saline Water and Gases in Crystalline rocks, Special Paper—Geological Association of Canada*, vol. 33 1987, pp. 111–119.
- Oren, O., Yechieli, Y., Böhlke, J.K., Dody, A., 2004. Contamination of groundwater under cultivated fields in an arid environment, central Arava Valley. *Isr. J. Hydrol.* 290, 312–328.
- Paquette, J.L., Nédélec, A., Moine, B., Rakotondrazafy, M., 1994. U–Pb single zircon Pb-evaporation and Sm–Nd isotopic study of granulite domain in SE Madagascar. *J. Geol.* 102, 523–538.
- Pili, E., Sheppard, S.M.F., Lardeaux, J.-M., Martelat, J.E., Nicolle, C., 1997. Fluid versus scale of shear zones in the lower continental crust and the granulite paradox. *Geology* 25, 15–18.
- Savadogo, A.N., 1984. *Géologie et hydrogéologie du socle cristallin de Haute Volta: étude régionale du bassin versant de la Sissili*. Doctoral Thesis. University of Grenoble, p. 350.
- Suk, H., Lee, K.K., 1999. Characterization of a groundwater hydrochemical system through multivariate analysis: clustering into ground water zones. *Ground Water* 37, 358–365.
- Thomas, J.M., Welch, A.H., Preissler, A.M., 1989. Geochemical evolution of groundwater in Smith Creek Valley—a hydrologically closed basin in Central Nevada, USA. *Appl. Geochem.* 4, 493–510.
- Traoré, A.Z., 1985. *Géologie et hydrogéologie des plateaux Mandingues (Mali). Région de Koula—Nossombougou*. Doctoral Thesis. University of Grenoble, p. 218.
- Travi, Y., Mudry, J., 1997. Assessing and managing nitrate contamination in Sahelian basement aquifers in West Africa. *Hydrogéologie* 1, 13–21.
- Windley, B.F., Bridgwater, D., 1971. The evolution of the Archaean low- and high-grade terrains. *Geol. Soc. Aust.* 3, 33–46.
- Wright, E.P., 1992. The hydrogeology of crystalline basement aquifers in Africa, *Geological Society Special Publication no. 66* 1992, p. 264.